European Journal of Medicinal Chemistry 59 (2013) 329–341

Contents lists available at SciVerse ScienceDirect

European Journal of Medicinal Chemistry

journal homepage: http://www.elsevier.com/locate/ejmech

Original article

Optimization of tocotrienols as antiproliferative and antimigratory leads

Fathy A. Behery, Mohamed R. Akl, Suryatheja Ananthula, Parash Parajuli, Paul W. Sylvester, Khalid A. El Sayed*

Department of Basic Pharmaceutical Sciences, College of Pharmacy, University of Louisiana at Monroe, 1800 Bienville Drive, Monroe, LA 71201, USA

ARTICLE INFO

Article history:
Received 9 July 2012
Received in revised form
20 October 2012
Accepted 10 November 2012
Available online 23 November 2012

Keywords:
Antimigratory
Antiproliferative
Breast cancer
In vitro
In vivo
1,3-Oxazine
Mannich
Lederer–Manasse
Tocotrienol

ABSTRACT

The vitamin E family members γ- and δ-tocotrienols (**2** and **3**, respectively) are known natural products with documented anticancer activities. Redox-silent structural modifications, such as esterification, etherification and carbamoylation, of **2** and **3** significantly enhanced their anticancer activities. However, hit-to-lead optimization of tocotrienols and their analogs was yet to be reported at the outset of the project described herein. Subjecting the chroman ring of **2** and **3** to the electrophilic substitution reactions, namely, Mannich and Lederer–Manasse procedures, afforded 42 new products. These included the 3,4-dihydro-1,3-oxazines **3**–**29** and **35**–**44**, Mannich bases **30**–**31**, and the hydroxymethyl analogs **32**–**34**. Of these, the δ-tocotrienol analogs **8**, **11**, **18**, **24**, **25**, **27**, and **40** inhibited the proliferation of the highly metastatic +SA mammary epithelial cancer cell line, with IC_{50} values in the nanomolar (nM) range. In NCI's 60 human tumor cell line panel, **8**, **17**, **38**, and **40** showed antiproliferative activity, with nM GI_{50} values. The δ-tocotrienol analogs **10** and **38** inhibited the migration of the highly metastatic human breast cancer cell line MDA-MB-231 with IC_{50} values of 1.3 and 1.5 μM, respectively, in the wound-healing assay. A dose of 0.5 mg/day for 14 days of one of the active analogs, **30**, significantly slowed the growth of +SA mammary tumors in the syngeneic BALB/c mouse model, compared to the vehicle- and the parent γ-tocotrienol-treated control groups. Electrophilic substitution reactions promoted tocotrienols to lead level and can enable their future use to control metastatic breast malignancies.

1. Introduction

The lipid-soluble vitamin E members are important antioxidants and essential nutrients for normal growth and development in animals [1]. Vitamin E is the generic name of tocopherols and tocotrienols that have the same general structure of methyl-substituted tocols. The term 'tocol' trivially refers to 2-methyl-2-(4,8,12-trimethyltridecyl)chroman-6-ol [2]. Tocotrienols, as the name implies, have three double bonds $\Delta^{3,7,11}$ with *E*-configuration in the tridecyl side chain, while tocopherols have a fully saturated phytyl side chain. The naturally occurring tocotrienol isomers (α-, β-, γ-, and δ-) differ in the number and position of the methyl groups on the 6-chromanol head [3].

Tocotrienols have better antioxidant activity than tocopherols [4,5]. In addition, tocotrienols exhibit a wide range of redox-silent biological activities in humans, independent of their radical-scavenging abilities [6]. This includes antiproliferative, antimigratory, anti-angiogenic, cholesterol-lowering, and neuroprotective activities [4,7]. These activities may be attributed to their unique modulatory effects on various intracellular signal transduction and gene expression pathways [4,5].

Structurally, tocotrienol skeleton can be divided into three domains correlated with biological activities. Domain I (phytyl side chain) docks the compound to the lipophilic membranes. Domain II (chroman ring) is responsible for vitamin E effects on different signaling enzymes. Finally, domain III (phenolic OH group) is responsible for the redox activity [8].

Different structural modifications of tocotrienols enhanced the in vitro anticancer activity. Domain III esterification, carbamoylation, and etherification resulted in products with improved anticancer activities [7,9–13]. The optimum length of domain I for proapoptotic activity was 2–3 isoprenyl units [13]. No reports for modifications of tocotrienols' domain II even though these modifications are expected to greatly affect the anticancer activity. This can be concluded based on the difference in the proapoptotic potency between tocotrienol isomers which differ in the number and position of the methyl groups on the chroman ring [13].

Phenols with unsubstituted *o*- or *p*-positions are sufficiently active to undergo electrophilic substitution reactions such as Mannich and Lederer–Manasse reactions [14]. Mannich reaction is

* Corresponding author. Tel.: +1 318 342 1725; fax: +1 318 342 1737.
E-mail address: elsayed@ulm.edu (K.A. El Sayed).

0223-5234/$ – see front matter © 2012 Elsevier Masson SAS. All rights reserved.
http://dx.doi.org/10.1016/j.ejmech.2012.11.012

extensively studied with phenols and naphthols, however only few publications dealt with tocopherols, not tocotrienols, as a reactive scaffold for this reaction to produce the corresponding Mannich base [15].

In Mannich reaction, the condensation of phenol, formaldehyde, and primary amine, is expected to produce multiple products, such as 3,4-dihydro-1,3-2H-benzoxazines, *o*-amino-methylphenols, or *N*,*N*-disubstituted amines. Phenol and the primary amine substituents along with the ratio of the reactants can determine the course of this reaction and subsequently the nature of the reaction products [16,17].

Mannich reaction products have been of great importance to pharmaceutical chemistry [18,19]. *N*-substituted-3,4-dihydro-2H-1,3-oxazines condensed with aromatic rings has various pharmacological effects such as antifungal and antitumor activities [20–24]. This study is the first report for the modifications of tocotrienols' domain II by electrophilic substitution reactions (Mannich and Lederer–Manasse reactions) and the assessment of the effect of such modifications on the antiproliferative and antimigratory activities, in vitro and in vivo.

2. Results and discussions

2.1. Chemistry

Both γ- and δ-tocotrienols (**1** and **2**, respectively) were isolated from a tocotrienol-rich fraction of palm oil using normal phase vacuum liquid chromatography [7]. Forty-two new tocotrienol analogs were prepared by electrophilic substitutions of the chroman ring.

2.1.1. Synthesis of tocotrienol analogs

In a Mannich-type reaction, the condensation of equimolar amounts of tocotrienol, primary amine, and formaldehyde produced the 3,4-dihydro-1,3-oxazine analogs **3**–**29**, **35**–**44**. However, using equimolar ratios of the reactants is expected to produce the Mannich bases [15,25]. In a primary amine, one hydrogen can be substituted to give the Mannich base, or the two hydrogen atoms can be substituted to give either the 3,4-dihydro-1,3-oxazine or *bis*-substituted tertiary amine [18,26]. In addition, the nature of the phenol and its substituents may play a major role in directing the reaction, regardless of the molar ratio of the reactants [17]. Both **1** and **2** were employed and they underwent the reaction successfully. Because **2** has two nonsubstituted *o*-positions (C-5 and C-7), two positional isomers were produced. The C-5 substituted product was predominant due to the higher reactivity of C-5 than C-7 site toward the electrophilic substitution reactions [3]. In addition, it is well established that the reaction takes place in the *o*-position α to the ring fusion in binuclear phenols that have the hydroxyl group in a β-position to the ring fusion [18]. Different aliphatic, alicyclic, and aralkyl primary amines were used with variable alkyl chain lengths and diverse terminal functional groups. The reaction did not proceed with secondary amines. The reaction proceeded toward the 1,3-oxazine formation regardless of the molar ratio of the reactants and their mixing order. The reaction was carried out either by mixing the primary amine, formaldehyde, and tocotrienol or condensing the amine and formaldehyde first and then the product was allowed to react with tocotrienol. Either dioxane or ethanol was used and occasionally the reaction was allowed to proceed under solvent-less conditions. Both aqueous formaldehyde and paraformaldehyde were satisfactorily used (Scheme 1a, b).

The Mannich bases were prepared from the corresponding 3,4-dihydro-1,3-oxazine analogs. **23** and **26** were shaken for 48 h at room temperature in 75% methanol solution to give the corresponding Mannich base (**30** and **31**, respectively) with the concomitant loss of one molecule of formaldehyde (Scheme 1c).

In Lederer–Manasse reaction [27], refluxing toluene solution of **1** with paraformaldehyde in presence of boric and acetic acids produced **32**, the 5-hydroxylmethyl analog of **1**. The hydroxymethylation of **2**, took place at either C-5 or C-7, producing **33** and **34**, respectively (Scheme 1d).

2.1.2. Structure elucidation

The HREIMS of **3** suggested the molecular formula $C_{31}H_{48}NO_2$ with nine degrees of unsaturation which inferred a new ring formation. The ^{1}H-NMR spectrum of **3** was identical to that of **1** [28], with the replacement of the aromatic proton signal of H-5 with three new singlet proton signals at δ_H 2.58, 3.76, and 4.67. In HMQC, The proton methyl singlet H_3-5″ (δ_H 2.58) was correlated to the new methyl carbon at δ_C 40.4. The other two proton signals, δ_H 3.76 (H_2-4″) and 4.67 (H_2-2″), were correlated to the methylene carbons at δ_C 50.5 and 83.0, respectively. In HMBC, the methyl H_3-5″ showed ^3J-HMBC correlations to carbon signals δ_C 50.5 (C-4″) and 83.0 (C-2″). Proton singlet H_2-4″ showed ^3J-HMBC correlations to the quaternary carbons at δ_C 145.2 (C-6) and 115.0 (C-9), in addition to a ^2J-HMBC correlation to C-2″. The methylene singlet H_2-2″ showed showed ^3J-HMBC correlations to C-6, C-4″, and C-5″. Although the reaction conditions and the molar ratio of the reactants would suggest the formation of a Mannich base [12,14], this spectral data indicate that **2** is not a Mannich base but (*R*)-2,5,6,8-tetramethyl-8-((3*E*,7*E*)-4,8,12-trimethyltrideca-3,7,11-trienyl)-1,2,3,8,9,10-hexahydrochromeno-[5,6-e] [1,3]oxazine. Extensive analyses of ^{1}H, ^{13}C (Tables 1–3, and S1–S8) and 2D NMR data along with the HRESIMS analysis confirmed the 3,4-dihydro-2H-1,3-oxazine ring formation in **4**–**29** and **35**–**44** in a similar fashion used with **3**. The oxazine ring is characterized by the two proton singlets, H-2″ and H-4″ at the range δ_H 4.30–4.88 and 3.76–3.95, respectively. C-2″ and C-4″ appears in the range of δ_C 79.9–83.4 and 44.8–50.5, respectively.

δ-Tocotrienol (**2**) reacted with 2-aminoethanol and HCHO, affording the isomers **10** (major) and **11** (minor). Both showed the characteristic two proton singlets and two methylenes of the oxazine ring. The spectroscopic identification of **10** as 2-((*R*)-6,8-dimethyl-8-((3*E*,7*E*)-4,8,12-trimethyltrideca-3,7,11-trienyl)-9,10-dihydrochromeno[5,6-e] [1,3]oxazin-2(1H,3H,8H)-yl)ethanol was achieved in a similar manner used for **3**. The aromatic proton singlet H-5 (δ_H 6.39, Table 3) in **11** showed ^3J-HMBC correlations to the quaternary aromatic carbons C-7 and C-10 (δ_C 123.4 and 146.0, respectively, Table 1). The proton singlet H_2-4″ (δ_H 3.90) showed ^3J-HMBC correlations to the quaternary aromatic carbons at δ_C 146.4 (C-6) and 120.5 (C-8), confirming the oxazine ring closure at C-7. Therefore **11** was proven to be 2-((*R*)-5,7-dimethyl-7-((3*E*,7*E*)-4,8,12-trimethyl-trideca-3,7,11-trienyl)-8,9-dihydrochromeno[7,6-e] [1,3]oxazin-3(2H,4H,7H)-yl)ethanol.

The HRESIMS of the Mannich base analogs **30** or **31** suggested molecular formula of $C_{39}H_{58}N\ O_4$ or $C_{37}H_{54}NO_3$, respectively, 12 mass units less than their parents **23** or **26**. This suggested the 1,3-oxazine hydrolytic ring opening with the loss of a formaldehyde molecule. This was confirmed by NMR data (Tables 1 and 2). The ^{1}H- and ^{13}C-NMR data for **30** and **31** were identical to those of their 3,4-dihydro-1,3-oxazine parents **23** and **26**, respectively, with the loss of the methylene proton and the carbon signals H_2/C-2″. The proton singlet H_2-1″ (δ_H 3.90) showed ^3J-HMBC correlations to the quaternary aromatic carbons at δ_C 147.7 (C-6) and 116.2 (C-8), confirming the oxazine ring opening and the attachment of the aminomethylene C-1″ to C-5. Therefore compounds **30** and **31** were confirmed to be (*R*)-5-((3,4-dimethoxyphenethyl-amino) methyl)-2,7,8-trimethyl-2-((3*E*,7*E*)-4,8,12-trimethyltrideca-3,7,11-trienyl)chroman-6-ol and (*R*)-5-((4-hydroxyphenethylamino)

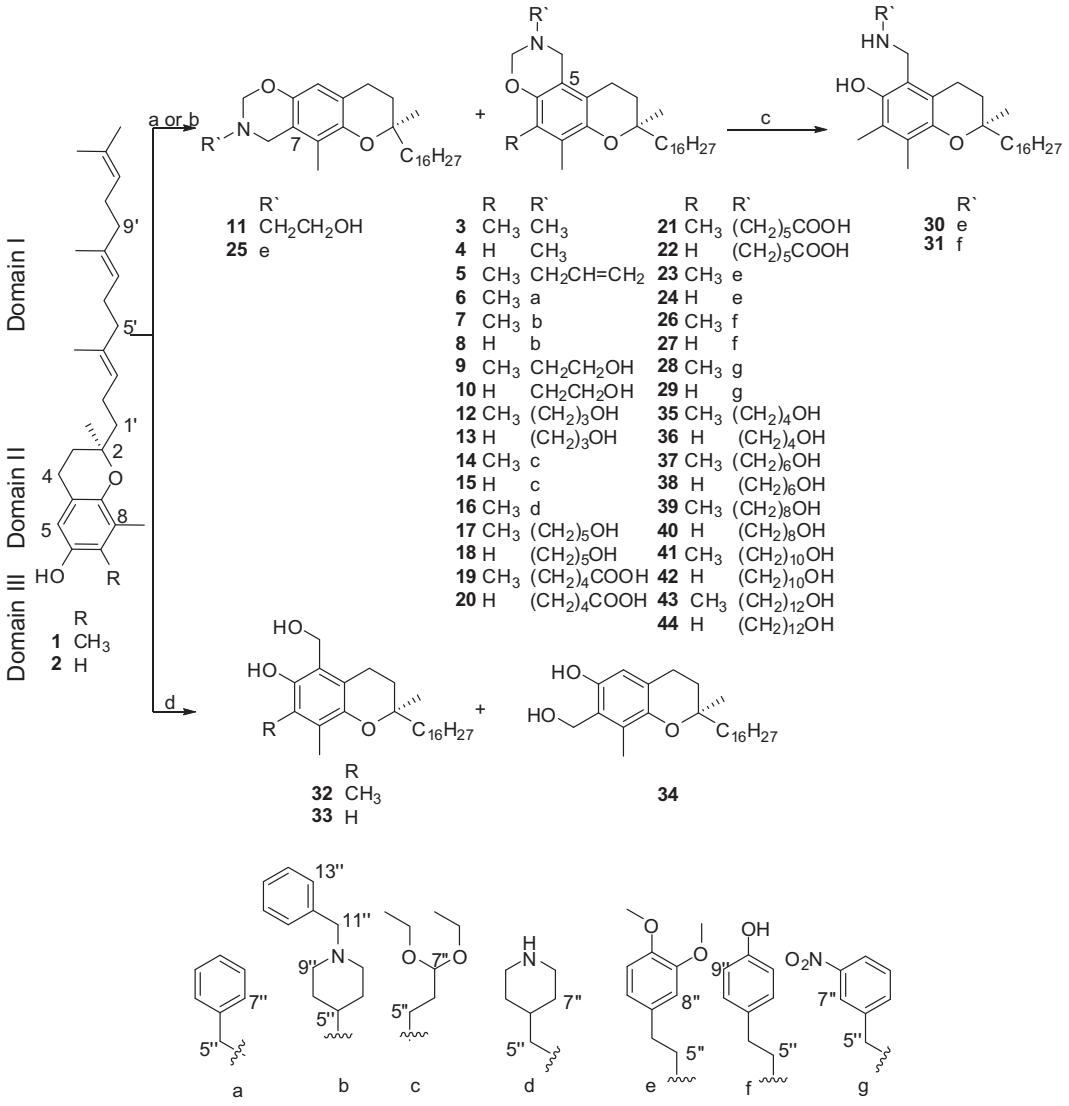

Scheme 1. Semisynthetic preparation of tocotrienol analogs. (a) 37% aq. CH_2O + RNH_2/dioxane, stirring, rt, 1 h, reflux, overnight. (b) $(CH_2O)_n$ + RNH_2, stirring, rt, overnight. (c) 200 mL 25% aq. MeOH, stirring, 48 h (d) $(CH_2O)_n$ + H_3BO_3 + CH_3COOH/toluene, reflux, overnight.

methyl)-2,7,8-trimethyl-2-((3*E*,7*E*)-4,8,12-trimethyltri-deca-3,7,11-trienyl)chroman-6-ol, respectively.

The HRESIMS of **32** suggested a molecular formula of $C_{29}H_{44}O_3$. The hydroxymethylene proton singlet H_2-1″ (δ_H 4.85, Table 3) showed ^3J-HMBC correlations to the quaternary aromatic carbons at δ_C 147.4 (C-6, Table 2) and 118.8 (C-9), in addition to a ^2J-HMBC correlation to the quaternary aromatic carbon at δ_C 115.2 (C-5). This confirmed the hydroxymethylation at C-5. Accordingly, **32** was confirmed to be (*R*)-5-(hydroxymethyl)-2,7,8-trimethyl-2-((3*E*,7*E*)-4,8,12-trimethyltri-deca-3,7,11-trienyl)chroman-6-ol. The HRESIMS of **33** and **34** suggested the same molecular formula $C_{28}H_{42}O_3$. Compound **33** was confirmed to be (*R*)-5-(hydroxymethyl)-2,8-dimethyl-2-((3*E*,7*E*)-4,8,12-trimethyltrideca-3,7,11-trienyl)chroman-6-ol, in a similar fashion to **32**. C-7 hydroxymethylation in case of **34** was confirmed through the ^3J-HMBC correlations of hydroxymethylene proton singlet H_2-1″ (δ_H 4.87, Table 3) to the quaternary aromatic carbons at δ_C 148.8 (C-6, Table 2) and 122.3 (C-8), the proton signal at was correlated to the carbon signal at δ_C 124.1 (C-7). Therefore, compound **34** was confirmed to be (*R*)-5-(hydroxymethyl)-2,7,8-trimethyl-2-((3*E*,7*E*)-4,8,12-trimethyltrideca-3,7,11-trienyl)chroman-6-ol.

2.2. Biological evaluations and structure–activity relationship

2.2.1. In vitro activities

2.2.1.1. Antiproliferative activity against the highly metastatic + SA mouse mammary epithelial cancer cells. The parent tocotrienols **1** and **2** effectively inhibited the proliferation of the highly metastatic +SA mammary epithelial cell line at IC_{50} values of 4.0 and 3.0 μM, respectively [29]. The antiproliferative activities of **3**–**44** against the abovementioned cells were evaluated by MTT assay and the IC_{50} values were calculated (Fig. 1, Table 4). Thirty out of 42 prepared compounds have shown IC_{50} values less than 3 μM, with better activity than δ-tocotrienol (**2**). Of these, seven compounds showed nanomolar IC_{50} values for the first time in the tocotrienol family (Table 4).

Generally, the oxazine analogs of **2** (δ-isomer) showed lower IC_{50} values than the corresponding analogs of **1** (γ-isomer). This pattern was consistent along most of the prepared oxazines except those with terminal CH_3CH_2O (**24**–**15**), COOH (**19**–**22**), or NO_2 (**28**–**29**) groups. However, this pattern was reversed in the Manasse–Lederer-based analogs **32**–**34**. The γ- isomer analog **32** showed lower IC_{50} value the than the δ-isomers **33** and **34**.

Table 1
^{13}C-NMR data of **3**, **10**, **11**, **23**, and **26**.[a]

δ_C, mult.	**3**	**10**	**11**	**23**	**26**
2	74.5, C	74.7, C	75.6, C	74.5, C	74.6, C
2-CH_3	23.9, CH_3	23.9, CH_3	24.2, CH_3	23.8, CH_3	23.9, CH_3
3	31.1, CH_2	31.0, CH_2	31.3, CH_2	31.1, CH_2	31.1, CH_2
4	18.9, CH_2	19.1, CH_2	22.3, CH_2	19.0, CH_2	18.9, CH_2
5	114.7, C	115.2, C	113.7, CH	115.0, C	114.8, C
6	145.2, C	146.3, C	146.4, C	145.2, C	145.2, C
7	124.0, C	116.4, CH	123.4, C	124.0, C	124.0, C
7-CH_3	11.4, CH_3	–	–	11.5, CH_3	11.5, CH_3
8	123.0, C	126.0, C	120.5, C	123.1, C	123.1, C
8-CH_3	11.7, CH_3	15.9, CH_3	10.5, CH_3	11.7, CH_3	11.7, CH_3
9	115.0, C	117.8, C	116.9, C	115.0, C	115.0, C
10	144.6, C	146.0, C	146.0, C	145.2, C	145.1, C
1′	39.8, CH_2	39.6, CH_2	39.9, CH_2	39.8, CH_2	39.2, CH_2
2′	22.3, CH_2	22.2, CH_2	22.4, CH_2	22.3, CH_2	22.3, CH_2
3′	124.5, CH	124.5, CH	124.5, CH	124.5, CH	124.5, CH
4′	135.2, C	135.3, C	135.3, C	135.2, C	135.2, C
4′-CH_3	16.1, CH_3	16.1, CH_3	16.1, CH_3	16.1, CH_3	16.1, CH_3
5′	39.8, CH_2	39.8, CH_2	39.8, CH_2	39.8, CH_2	39.2, CH_2
6′	26.8, CH_2	26.8, CH_2	26.8, CH_2	26.8, CH_2	26.8, CH_2
7′	124.4, CH	124.3, CH	124.3, CH	124.4, CH	124.4, CH
8′	135.0, C	135.1, C	135.1, C	135.1, C	135.1, C
8′-CH_3	11.7, CH_3	16.0, CH_3	16.0, CH_3	16.0, CH_3	16.0, CH_3
9′	39.8, CH_2	39.8, CH_2	39.8, CH_2	39.8, CH_2	39.2, CH_2
10′	26.7, CH_2	26.7, CH_2	26.7, CH_2	26.7, CH_2	26.7, CH_2
11′	124.3, CH	124.2, CH	124.2, CH	124.3, CH	124.3, CH
12′	131.3, C	131.4, C	131.4, C	131.4, C	132.1, C
12′a-CH_3	17.8, CH_3	17.8, CH_3	17.8, CH_3	17.8, CH_3	17.8, CH_3
12′b-CH_3	25.8, CH_3	25.8, CH_3	25.8, CH_3	25.8, CH_3	25.8, CH_3
2″	83.0, CH_2	81.9, CH_2	81.6, CH_2	81.7, CH_2	81.5, CH_2
4″	50.5, CH_2	47.9, CH_2	48.7, CH_2	48.8, CH_2	48.8, CH_2
5″	40.4, CH_3	53.9, CH_2	53.9, CH_2	53.8, CH_2	53.9, CH_2
6″		59.2, CH_2	58.9, CH_2	34.8, CH_2	34.0, CH_2
7″				132.7, C	131.3, C
8″				112.0, CH	129.8, CH
9″				148.9, C	115.3, CH
10″				147.5, C	154.1, C
11″				111.3, CH	115.3, CH
12″				120.6, CH	129.8, CH
13″				56.0, CH_3	
14″				56.0, CH_3	

[a] In $CDCl_3$, 100 MHz. Carbon multiplicities were determined by APT experiments, C, quaternary; CH, methine; CH_2, methylene; CH_3, methyl carbons.

Table 2
^{13}C-NMR data of **30**–**34**.[a]

δ_C, mult.					
Position	**30**	**31**	**32**	**33**	**34**
2	74.1, C	74.2, C	74.4, C	74.5, C	75.5, C
2-CH_3	23.7, CH_3	23.7, CH_3	23.8, CH_3	23.8, CH_3	24.1, CH_3
3	31.6, CH_2	31.6, CH_2	31.5, CH_2	31.4, CH_2	31.3, CH_2
4	20.4, CH_2	20.4, CH_2	19.9, CH_2	19.9, CH_2	22.3, CH_2
5	115.5, C	116.2, C	115.2, C	118.3, C	113.7, CH
6	147.7, C	149.0, C	147.4, C	148.3, C	148.8, C
7	123.0, C	125.0, C	125.9, C	116.8, CH	124.1, C
7-CH_3	11.8, CH_3	11.9, CH_3	11.5, CH_3	–	–
8	124.9, C	123.1, C	123.1, C	127.3, C	122.3, C
8-CH_3	12.0, CH_3	12.0, CH_3	12.0, CH_3	15.9, CH_3	11.2, CH_3
9	116.2, C	116.2, C	118.8, C	119.9, C	121.3, C
10	144.2, C	144.3, C	144.9, C	145.5, C	145.3, C
1′	39.8, CH_2	39.7, CH_2	39.5, CH_2	39.5, CH_2	39.8, CH_2
2′	22.3, CH_2	22.3, CH_2	22.3, CH_2	22.2, CH_2	22.5, CH_2
3′	124.4, CH	124.5, CH	124.5, CH	124.5, CH	124.5, CH
4′	135.2, C	135.2, C	135.2, C	135.3, C	135.2, C
4′-CH_3	16.1, CH_3	16.1, CH_3	16.0, CH_3	16.2, CH_3	16.0, CH_3
5′	39.8, CH_2	39.7, CH_2	39.8, CH_2	39.8, CH_2	39.8, CH_2
6′	26.8, CH_2	26.8, CH_2	26.8, CH_2	26.8, CH_2	26.8, CH_2
7′	124.3, CH	124.4, CH	124.4, CH	124.3, CH	124.3, CH
8′	135.0, C	135.1, C	135.1, C	135.1, C	135.1, C
8′-CH_3	16.0, CH_3	16.0, CH_3	15.9, CH_3	16.1, CH_3	15.9, CH_3
9′	39.8, CH_2	39.7, CH_2	39.8, CH_2	39.8, CH_2	39.8, CH_2
10′	26.7, CH_2	26.7, CH_2	26.7, CH_2	26.7, CH_2	26.7, CH_2
11′	124.3, CH	124.3, CH	124.3, CH	124.3, CH	124.2, CH
12′	131.4, C	131.4, C	131.3, C	131.4, C	131.4, C
12′a-CH_3	17.8, CH_3	17.8, CH_3	17.5, CH_3	17.8, CH_3	17.8, CH_3
12′b-CH_3	25.8, CH_3	25.8, CH_3	25.8, CH_3	25.8, CH_3	25.8, CH_3
1″	47.6, CH_2	47.4, CH_2	60.1, CH_2	59.6, CH_2	60.6, CH_2
3″	50.0, CH_2	49.9, CH_2			
4″	35.6, CH_2	34.9, CH_2			
5″	131.8, C	130.8, C			
6″	111.9, CH	129.9, CH			
7″	149.3, C	115.6, CH			
8″	149.1, C	154.6, C			
9″	111.4, CH	115.6, CH			
10″	120.7, CH	129.9, CH			
11″	56.0, CH_3				
12″	55.9, CH_3				

[a] In $CDCl_3$, 100 MHz. Carbon multiplicities were determined by APT experiments, C, quaternary; CH, methine; CH_2, methylene; CH_3, methyl carbons.

Extending the length of the N-3″ substituent (up to 8-carbons) proved to enhance the activity. In addition, a terminal OH group at N-3″ substituent was preferred for the activity over the COOH (**20**), NH (**16**), or NO_2 (**28**, Fig. 2). Masking the OH by etherification did not affect the activity (**23**, **24**, **15**) except in **14**, whose activity was significantly decreased (Table 4).

2.2.1.2. The antiproliferative and cytotoxic activities against the National Cancer Institute (NCI) 60 human cell lines panel. The growth inhibitory activity of twenty compounds, eighteen oxazines (**8**, **13**, **17**, **18**, **23**, **24**, **26**, **27**, and **35**–**44**) and two Mannich bases (**30** and **31**), was evaluated against the National Cancer Institute's panel of 60 human cell lines (NCI-60) at a single dose of 10 μM (Fig. SI1). The growth inhibition activity of these compounds, except **23**, **26**, **30**, and **31**, have been evaluated at five different doses (100, 10, 0.1, 0.01, 0.001 μM). The GI_{50} values, the concentrations that inhibit the growth of 50% of the cell, were calculated (Fig. SI2). Compounds **13**, **36**, **38**, and **40** were lethal to the cells at 10 μM dose, showing negative mean percent growth values across all 60 cell lines (mean60), while **1** was inactive (Fig. 3). It was obvious from the mean60 values that the oxazine ring was essential pharmacophore required for the activity since the Mannich bases **30** and **31**, without the oxazine ring, were showing the same activity as **1**. The mean60 was decreasing by increasing the length of the N-3″ substituent from 4-carbons (**36**), 6-carbons (**38**), and 8-carbons (**40**). However, increasing the length of the N-3″ substituent to 12-carbons, led to reducing the activity and increasing the mean60 value. This may indicate that the optimal length of the N-3″ substituent for best activity was 8-carbons. Comparison of the mean60 values for γ- and δ-isomers substituents indicate that the oxazine analogs of **2** (δ-isomer) were more cytotoxic or growth inhibitors than the corresponding **1** analogs (γ-isomer, Fig. 3). Representing the data in the form of mean graphs, in which the percent growth of each cell line is subtracted from the mean60, enables the detection of the differential growth inhibition activity of the compound on different tumor tissues and cell lines. Tocotrienol analogs showed selective growth inhibition of blood and colon malignant cell lines (Fig. 4). Compounds **8**, **17**, **38**, and **40** inhibited the growth of leukemia and colon cancer cell lines at nanomolar GI_{50} values (Fig. SI2). This selectivity pattern to leukemia and colon cell lines was further confirmed when IC_{50} values of the growth inhibitory activity of some of the tocotrienol analogs were determined by MTT assay against the human breast cancer cell lines MDA-MB-231 and MCF7 (Table 5).

2.2.1.3. Antiproliferative activity against the non-tumorigenic MCF10A epithelial cell line. Compound **1**, along with ten tocotrienol analogs which showed the high potencies against the highly metastatic +SA cell line, were then tested against the non-tumorigenic MCF10A human mammary epithelial cells in order to

Table 3
^{1}H-NMR data of **3**, **10**, **11**, **23**, **26**, **30**–**34**.[a]

δ_H, mult., *J*										
Position	**3**	**10**	**11**	**23**	**26**	**30**	**31**	**32**	**33**	**34**
2-CH_3	1.24, s	1.25, s	1.25, s	1.24, s	1.24, s	1.20, s	1.21, s	1.23,s	1.23, s	1.24, s
3	1.78, m	1.67, m	1.75, m	1.75, m	1.77, m	1.74, m	1.74, m	1.77, m	1.74, m	1.74, m
4	2.44, m	2.45, m	2.69, m	2.43, m	2.42, m	2.56, t, 6.9	2.57, t, 6.4	2.62, m	2.60, m	2.68, m
5			6.39, s							6.44, s
7		6.49, s							6.51, s	
7-CH_3	2.10, s			2.10, s	2.10, s	2.13, s	2.13, s	2.15, s		
8-CH_3	2.10, s	2.12, s	1.98, s	2.09, s	2.09, s	2.09, s	2.09, s	2.11, s	2.10, s	2.10, s
1′	1.54, m	1.55, m	1.52, m	1.55, m	1.55, m	1.52, m	1.52, m	1.52, m	1.52, m	1.53, m
2′	2.07, m	2.14, m	2.11, m	2.12, m	2.14, m	2.10, m	2.11, m	2.12, m	2.10, m	2.09, m
3′	5.13, m	5.09, m	5.10, m	5.11, m	5.10, m	5.08, m	5.08, m	5.11, m	5.10, m	5.08, m
4′-CH_3	1.59, s	1.59, s	1.59, s	1.59, s	1.60, s	1.57, s	1.57, s	1.59, s	1.58, s	1.58, s
5′	1.97, m	1.96, m	1.96, m	1.97, m	1.97, m	1.94, m	1.96, m	1.96, m	1.98, m	1.96, m
6′	2.05, m	2.05, m	2.04, m	2.05, m	2.05, m	2.03, m	2.04, m	2.05, m	2.05, m	2.04, m
7′	5.13, m	5.09, m	5.10, m	5.11, m	5.10, m	5.08, m	5.08, m	5.11, m	5.10, m	5.08, m
8′-CH_3	1.59, s	1.59, s	1.59, s	1.59, s	1.60, s	1.57, s	1.57, s	1.59, s	1.58, s	1.58, s
9′	1.97, m	1.96, m	1.96, m	1.97, m	1.97, m	1.94, m	1.96, m	1.96, m	1.98, m	1.96, m
10′	2.05, m	2.05, m	2.04, m	2.05, m	2.05, m	2.03, m	2.04, m	2.05, m	2.05, m	2.04, m
11′	5.13, m	5.09, m	5.10, m	5.11, m	5.10, m	5.08, m	5.08, m	5.11, m	5.10, m	5.08, m
12'a-CH_3	1.59, s	1.58, s	1.58, s	1.58, s	1.58, s	1.56, s	1.58, s	1.58, s	1.58, s	1.58, s
12'b-CH_3	1.67, s	1.67, s	1.67, s	1.67, s	1.68, s	1.65, s	1.66, s	1.67, s	1.67, s	1.67, s
1″						3.89, s	3.89, s	4.85, s	4.79, s	4.87, s
2″	4.67, s	4.74, s	4.75, s	4.78, s	4.78, s					
3″						2.91, t, 7.3	2.88, t, 7.1			
4″	3.76, s	3.84, s	3.90, s	3.85, s	3.84, s	2.77, t, 6.4	2.74, t, 6.9			
5″	2.58, s	2.95, t, 5.1	2.95, t, 5.1	2.99, t, 6.22	2.98, t, 7.7					
6″		3.67, t, 5.2	3.68, t, 4.8	2.85, t, 6.42	2.82, t, 7.7	6.69, d, 1.8	7.01, d, 8.2			
7″							6.74, d, 8.7			
8″				6.74–6.77, m	7.06, d, 8.4					
9″					6.71, d, 8.4	6.78, d, 7.8	6.74, d, 8.7			
10″						6.72, dd, 1.8, 8.2	7.01, d, 8.2			
11″				6.74–6.77, m	6.71, d, 8.4	3.86, s or 3.84, s				
12″				6.74–6.77, m	7.06, d, 8.4	3.86, s or 3.84, s				
13″				3.86, s						
14″				3.84, s						

[a] In $CDCl_3$, *J* in Hz. 400 MHz.

investigate their selectivity for tumor cells over normal cells. All tested tocotrienol analogs, except **23**, showed higher selectivity for + SA cells than for MCF10A (Table 7). The selectivity indices of tocotrienol analogs were higher than the parent compound **1** (selectivity index = 1.1, Table 7).

2.2.1.4. Antimigratory activity against the highly metastatic MDA-MB-231 breast cancer cell line. Tocotrienols were reported to inhibit the metastasis and invasion of gastric adenocarcinoma, melanoma, prostate, as well as breast cancer cell lines [7,9,30–32]. The wound-healing assay (WHA) is a simple method for the study of in vitro cell migration [7]. The antimigratory activities of the prepared compounds were evaluated against the highly metastatic MDA-MB-231 human breast cancer cells (Fig. 5). The concentrations required to inhibit the migration of 50% of the cells across the wound, IC_{50} values, were calculated (Table 6). The parent tocotrienols **1** and **2** showed limited activity against this aggressive cell line with IC_{50} values more than 40 μM. The 1,3-oxazine analogs are more active than both the Mannich bases and the hydroxymethyl derivatives as antimigratory agents. A terminal OH group, alcoholic

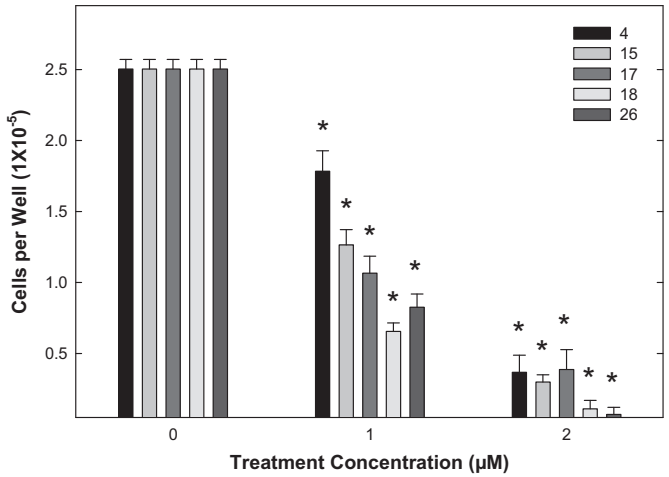

Fig. 1. Effect of tocotrienol analogs **4**, **15**, **17**, **18**, and **26** on the viability of +SA mammary tumor cells. $P < 0.05$ as respect to each compound respective vehicle treatment control (0 μM).

Table 4
Antiproliferative activity of tocotrienol analogs against the highly metastatic +SA mouse mammary epithelial cancer cell line.[a]

Compound	IC_{50} (μM)	Compound	IC_{50} (μM)	Compound	IC_{50} (μM)
3	2.2	**17**	1.7	**31**	2.3
4	1.3	**18**	0.70	**32**	2.6
5	11.6	**19**	1.8	**33**	>20
6	2.0	**20**	11.9	**34**	6.6
7	8.7	**21**	5.0	**35**	2.2
8	0.8	**22**	5.1	**36**	1.8
9	1.7	**23**	1.8	**37**	2.1
10	4.2	**24**	0.87	**38**	1.3
11	0.96	**25**	0.84	**39**	1.4
12	2.5	**26**	1.5	**40**	0.79
13	1.8	**27**	0.91	**41**	4.4
14	9.3	**28**	24.6	**42**	3.6
15	1.0	**29**	29.1	**43**	>5.0
16	4.6	**30**	1.7	**44**	2.0

[a] The IC_{50} values are calculated by non-linear regression fitting using GraphPad Prism 5.04.

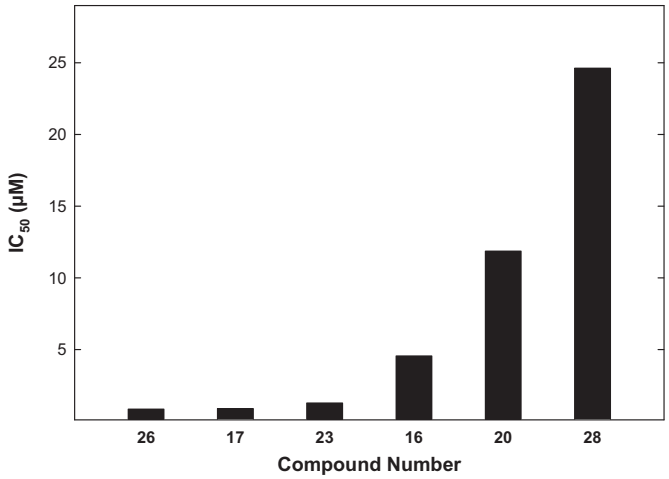

Fig. 2. The effect of the terminal group at N-3″ substituent on the viability of +SA mammary tumor cells. Free OH (**17** and **26**) or OCH_3 (**23**) > NH (**16**) > COOH (**20**) > NO_2 (**28**).

or phenolic, is important for the activity. The oxazine analogs of **2** (δ-isomer) were more active than the corresponding analogs of **1** (γ-isomer) as antimigratory agents. The most active compounds were **10**, **38**, **36**, and **27** with IC_{50} values of 1.3, 1.5, 2.2, and 2.4 μM, respectively (Table 6). Compounds **10**, **38**, and **36** possess linear aliphatic ethanol, hexanol, or butanol side chains attached to N-3″. This clearly shows the preference of a terminal free hydroxy functionality at 2–6 carbons distance from N-3″. The only analog among the most active compounds with aromatic (tyramine) side chain (**27**) can still be envisioned as a 6-carbons chain separating the free phenol hydroxy and N-3″. Therefore, these compounds can be considered as potential hits appropriate for optimization as antimetastatic agents.

2.2.2. In vivo activity

The effects of daily iv treatment with 0 or 0.5 mg of the parent compound **1** or **30** dissolved in 0.1 mL propylene glycol on +SA mammary tumor growth in syngeneic BALB/c mice is shown in Fig. 6. Palpable +SA mammary tumors started to appear in all groups approximately 40 days following tumor cell injection into the #4 mammary gland fat pad. Measurable tumors continued to grow throughout the 14-day treatment period in the vehicle- and

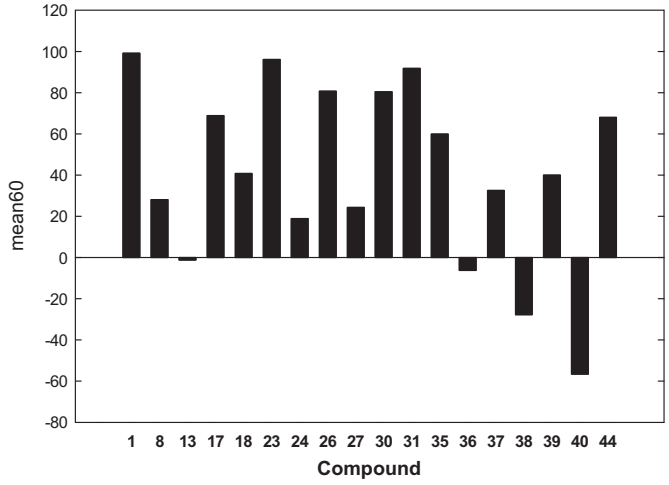

Fig. 3. The mean percent growth activity of the compounds **1**, **8**, **13**, **17**, **18**, **23**, **24**, **26**, **27**, **30**, **31**, **35**–**40**, **44** across all the 60 cell lines (mean60). The negative values indicate cytotoxicity.

1-treated control groups. In contrast, +SA mammary tumors in animals receiving 0.5 mg/day of compound **30** grew at a significantly slower rate, as compared to tumors in the vehicle control- and **1**-treated groups (Fig. 6). Body weights did not significantly differ among the different treatment groups at any time during the 14-day treatment experimental period.

This remarkable improvement in tocotrienol activity both in vitro and in vivo by the introduction of the new carbon–carbon bond through Mannich-based reaction opens new horizons for future hit-to-lead development of tocotrienol analogs as potential drugs to control metastatic breast cancer.

3. Conclusions

New 42 tocotrienol 3,4-dihydro-1,3-oxazine, Mannich base and hydroxymethyl analogs were prepared. The 3,4-dihydro-1,3-oxazine ring together with N-3″ substituent were important pharmacophores for the antiproliferative and antimigratory activities of the newly prepared tocotrienol analogs. In addition, the degree of methylation of the chroman ring has shown to affect the activities in a significant way. Modifications of domain II of tocotrienols by electrophilic substitution reactions can selectively improve not only the in vitro antiproliferative and antimigratory activities with minimal toxicity to normal cells but also the in vivo tumor growth inhibition activities of these compounds. This study shows the potential of tocotrienol as scaffold candidates for use to design future drugs for the control of metastatic breast cancer.

4. Materials and methods

4.1. Chemistry

All reagents and chemicals were purchased from Sigma–Aldrich Chemical Co. Tocotrienol-rich fraction 50 g (Palm TRF 70%, low in tocopherol from First Tech International Ltd., Hong Kong) was fractionated on Si gel 60 using *n*-hexane-ethyl acetate (gradient elution). Optical rotations were measured on a Rudolph Research Analytical Autopol III polarimeter. IR spectra were recorded on a Varian 800 FT-IR spectrophotometer. The ^{1}H- and ^{13}C-NMR spectra were recorded in $CDCl_3$, using TMS as an internal standard, on a JEOL Eclipse-400 NMR spectrometer, operating at 400 MHz for ^{1}H and 100 MHz for ^{13}C. The HREIMS experiments were conducted at Louisiana State University on a 6200-TOF LCMS (Agilent) equipped with multimode source (mixed source that can ionized the compounds alternatively by ESI and APCI). The ESIMS was conducted using 3200 Q-trap LC/MS/MS system (Applied Biosystems, Foster City, CA) using Analyst version 1.4.1 software (MDS Sciex; Toronto, Canada). The analytes were ionized using electrospray ionization (ESI) interface operated in the positive mode. The analysis was conducted using Q1 scan and mass scan range was *m*/*z* 50–500 (0.15 s/scan). TLC analysis was carried on precoated Si gel 60 F_{254} 500 μm TLC plates (EMD Chemicals), using variable proportions of *n*-hexane–ethyl acetate and ethyl acetate–methanol–water as a mobile phase. Vanillin in concentrated H_2SO_4 (1% w/v) was used as visualizing reagent. For column chromatography, Si gel 60 (Natland, 63–200 μm) was used.

4.2. General procedure for the preparation of 3,4-dihydro-2H-1,3-oxazines (*3*–*29* and *35*–*44*)

4.2.1. Method A

To a dioxane [15] solution (5 mL) of tocotrienol (4 mmol), the amine (20 mmol) was added. Mixture was cooled in an ice bath and 37% formaldehyde (21 mmol) was added drop wise while stirring. It was then stirred at room temperature for 1 h and then refluxed

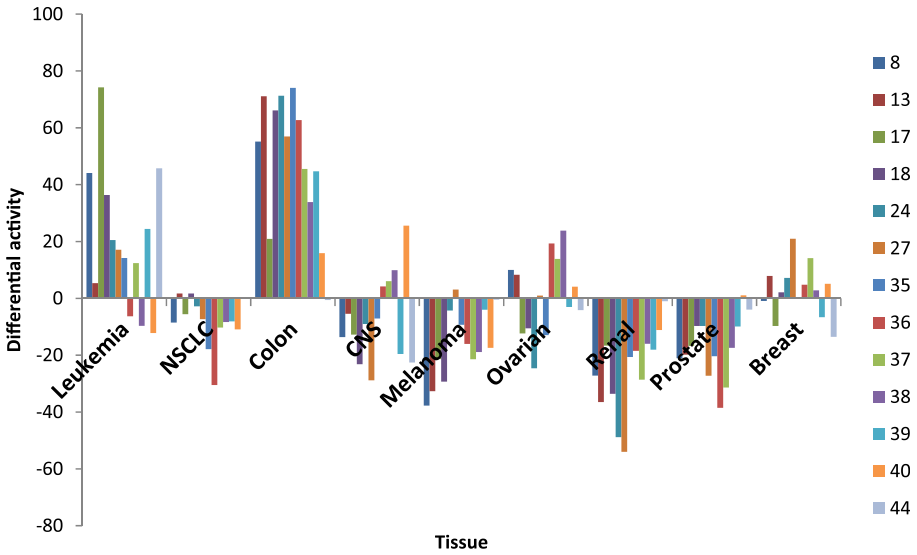

Fig. 4. The selectivity pattern of tocotrienol analogs on the cell lines belonging to different tissues. The selectivity is calculated by subtracting the mean growth percent of each tissue from the mean60. A positive value indicates selectivity.

overnight. Reaction mixture was concentrated under vacuum and the yellow residue obtained was dissolved in ethyl acetate (20 mL), washed several times with saturated NaCl solution, dried over anhydrous $MgSO_4$, and concentrated in vacuum. The residue obtained was subjected to column chromatography using normal phase silica gel as stationary phase and gradient ethyl acetate/*n*-hexane system as mobile phase (Scheme 1a).

4.2.2. Method B

A mixture of tocotrienol [25] (5.0 mmol), paraformaldehyde (5.0 mmol) and amines (5.0 mmol) was stirred and left overnight at rt. The reaction was carried out under solvent-less conditions (few drops of dioxane or ethanol may be added). The residue was purified by flash chromatography directly from the reaction mixture without any work-up (Scheme 1b).

Table 5
Antiproliferative activity (IC_{50}, μM) of tocotrienol analogs against the highly metastatic MDA-MB-231 and MCF7 human cancer cell lines and the non-tumorigenic MCF10A epithelial cell line.[a]

Compound	MCF7	MDA-MB-231
1	7.1	9.4
6	>20.0	27.3
10	6.0	>5.0
12	>20.0	9.6
13	>20.0	>10.0
16	>20.0	0.8
17	>20.0	>50.0
18	9.1	9.0
23	>20.0	>50.0
26	10.6	>5.0
27	18.2	>5.0
35	>20.0	13.8
36	16.3	>5.0
37	>20.0	>10.0
38	>20.0	>5.0
39	>20.0	>20.0
40	>20.0	11.7
41	19.4	15.7
42	4.6	12.4
43	>20.0	>50.0
44	>20.0	>50.0

[a] The IC_{50} values are calculated by non-linear regression fitting using GraphPad Prism 5.04.

*4.2.3. (R)-2,5,6,8-tetramethyl-8-((3E,7E)-4,8,12-trimethyltrideca-3,7,11-trienyl)-1,2,3,8,9,10-hexahydrochromeno[5,6-e] [1,3]oxazine (**3**)*

Yellow viscous oil, $[\alpha]_D^{25}$ +1.7 (*c* 0.016, CH_2Cl_2); IR (CH_2Cl_2)ν_{max} 3599, 2975, 2926, 1605 cm^{-1}; ^{1}H- and ^{13}C-NMR: see Tables 1 and 3; HREIMS *m*/*z* 466.3664, $[M + H]^+$ (calcd for $C_{31}H_{48}NO_2$, 466.3680).

*4.2.4. (R)-2,6,8-trimethyl-8-((3E,7E)-4,8,12-trimethyltrideca-3,7,11-trienyl)-1,2,3,8,9,10-hexahydrochromeno[5,6-e] [1,3]oxazine (**4**)*

Yellow viscous oil, $[\alpha]_D^{25}$ +4.7 (*c* 0.024, CH_2Cl_2); IR (CH_2Cl_2)ν_{max} 3660, 22858, 1618, 1476, 1345, 1099, 942 cm^{-1}; ^{1}H- and ^{13}C-NMR: see Tables S1 and S5; HREIMS *m*/*z* 452.6907, $[M + H]^+$ (calcd for $C_{30}H_{46}NO_2$, 452.6917).

*4.2.5. (R)-2-allyl-5,6,8-trimethyl-8-((3E,7E)-4,8,12-trimethyltrideca-3,7,11-trienyl)-1,2,3,8,9,10-hexahydrochromeno[5,6-e] [1,3]oxazine (**5**)*

Yellow viscous oil, $[\alpha]_D^{25}$+0.1 (*c* 0.03, CH_2Cl_2); IR (CH_2Cl_2)ν_{max} 3676, 2923, 1606 cm^{-1}; ^{1}H- and ^{13}C-NMR: see Tables S1 and S5; HREIMS *m*/*z* 492.3843, $[M + H]^+$ (calcd for $C_{33}H_{50}NO_2$,492.3836).

*4.2.6. (R)-2-benzyl-5,6,8-trimethyl-8-((3E,7E)-4,8,12-trimethyltrideca-3,7,11-trienyl)-1,2,3,8,9,10-hexahydrochromeno [5,6-e] [1,3]oxazine (**6**)*

Yellow viscous oil, $[\alpha]_D^{25}$+0.6 (*c* 0.04, CH_2Cl_2); IR (CH_2Cl_2)ν_{max} 3600, 2927, 2850, 1605 cm^{-1}; ^{1}H- and ^{13}C-NMR: see Tables S1 and S5; HREIMS *m*/*z* 542.3980, $[M + H]^+$ (calcd for $C_{37}H_{52}NO_2$, 542.3993).

*4.2.7. (R)-2-(1-benzylpiperidin-4-yl)-5,6,8-trimethyl-8-((3E,7E)-4,8,12-trimethyltrideca-3,7,11-trienyl)-1,2,3,8,9,10-hexahydrochromeno[5,6-e] [1,3]oxazine (**7**)*

Yellow viscous oil, $[\alpha]_D^{25}$+0.2 (*c* 0.047, CH_2Cl_2); IR (CH_2Cl_2)ν_{max} 3599, 2928, 1605, 1378 cm^{-1}; ^{1}H- and ^{13}C-NMR: see Tables S1 and S5; HREIMS *m*/*z* 625.4733, $[M + H]^+$ (calcd for $C_{42}H_{61}N_2O_2$, 625.4728).

*4.2.8. (R)-2-(1-benzylpiperidin-4-yl)-6,8-dimethyl-8-((3E,7E)-4,8,12-trimethyltrideca-3,7,11-trienyl)-1,2,3,8,9,10-hexahydrochromeno[5,6-e] [1,3]oxazine (**8**)*

Yellow viscous oil, $[\alpha]_D^{25}$+0.2 (*c* 0.083, CH_2Cl_2); IR (CH_2Cl_2)ν_{max} 3684, 2927, 1605, 1474 cm^{-1}; ^{1}H- and ^{13}C-NMR: see Tables S1 and

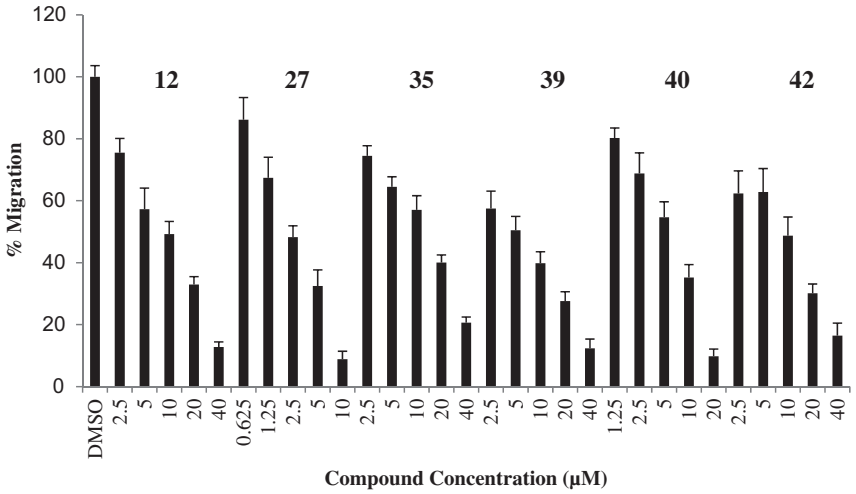

Fig. 5. Dose–response antimigratory activity of **12**, **27**, **35**, **39**, **40**, and **42** against the highly metastatic MDA-MB-231 human breast cancer cells in wound-healing assay.

S5; HREIMS *m/z* 611.4581, $[M + H]^+$ (calcd for $C_{41}H_{59}N_2O_2$, 611.4571).

*4.2.9. 2-((R)-5,6,8-trimethyl-8-((3E,7E)-4,8,12-trimethyltrideca-3,7,11-trienyl)-9,10-dihydrochromeno[5,6-e] [1,3]oxazin-2(1H,3H,8H)-yl)ethanol (**9**)*

Yellow viscous oil, $[\alpha]_D^{25}$+66.0 (*c* 0.0008, CH_2Cl_2); IR (CH_2Cl_2)ν_{max} 3602, 2850, 1605, 1091 cm^{-1}; ^1H- and ^{13}C-NMR: see Tables S1 and S5; HREIMS *m/z* 496.3769, $[M + H]^+$ (calcd for $C_{32}H_{50}NO_3$, 496.3785).

*4.2.10. 2-((R)-6,8-dimethyl-8-((3E,7E)-4,8,12-trimethyltrideca-3,7,11-trienyl)-9,10-dihydrochromeno[5,6-e] [1,3]oxazin-2(1H,3H,8H)-yl)ethanol (**10**)*

Yellow viscous oil, $[\alpha]_D^{25}$+0.2 (*c* 0.06, CH_2Cl_2); IR (CH_2Cl_2)ν_{max} 3599, 2928, 2855, 1606, 1473 cm^{-1}; ^1H- and ^{13}C-NMR: see Tables 1 and 3; HREIMS *m/z* 482.3632, $[M + H]^+$ (calcd for $C_{31}H_{48}NO_3$, 482.3629).

*4.2.11. 2-((R)-5,7-dimethyl-7-((3E,7E)-4,8,12-trimethyltrideca-3,7,11-trienyl)-8,9-dihydrochromeno[7,6-e] [1,3]oxazin-3(2H,4H,7H)-yl)ethanol (**11**)*

Yellow viscous oil, $[\alpha]_D^{25}$+24.0 (*c* 0.018, CH_2Cl_2); IR (CH_2Cl_2)ν_{max} 3599, 2996, 1606, 1292, 1241 cm^{-1}; ^1H- and ^{13}C-NMR: see Tables 1 and 3; HREIMS *m/z* 482.3620, $[M + H]^+$ (calcd for $C_{31}H_{48}NO_3$, 482.3629).

*4.2.12. 3-((R)-5,6,8-trimethyl-8-((3E,7E)-4,8,12-trimethyltrideca-3,7,11-trienyl)-9,10-dihydrochromeno[5,6-e] [1,3]oxazin-2(1H,3H,8H)-yl)propan-1-ol (**12**)*

Yellow viscous oil, $[\alpha]_D^{25}$+1.7 (*c* 0.03, CH_2Cl_2); IR (CH_2Cl_2)ν_{max} 3599, 1647, 1289, 1242 cm^{-1}; ^1H- and ^{13}C-NMR: see Tables S1 and S5; HREIMS *m/z* 510.3949, $[M + H]^+$ (calcd for $C_{33}H_{52}NO_3$, 510.3942).

*4.2.13. 3-((R)-6,8-dimethyl-8-((3E,7E)-4,8,12-trimethyltrideca-3,7,11-trienyl)-9,10-dihydrochromeno[5,6-e] [1,3]oxazin-2(1H,3H,8H)-yl)propan-1-ol (**13**)*

Yellow viscous oil, $[\alpha]_D^{25}$+0.2 (*c* 0.05, CH_2Cl_2); IR (CH_2Cl_2)ν_{max} 3599, 2929, 1606 cm^{-1}; ^1H- and ^{13}C-NMR: see Tables S1 and S5; HREIMS *m/z* 496.3783, $[M + H]^+$ (calcd for $C_{32}H_{50}NO_3$, 496.3785).

*4.2.14. (R)-2-(3,3-diethoxypropyl)-5,6,8-trimethyl-8-((3E,7E)-4,8,12-trimethyltrideca-3,7,11-trienyl)-1,2,3,8,9,10-hexahydrochromeno[5,6-e] [1,3]oxazine (**14**)*

Yellow viscous oil, $[\alpha]_D^{25}$+21.5 (*c* 0.0011, CH_2Cl_2); IR (CH_2Cl_2)ν_{max} 3599, 2922, 2853, 1606, 1374, 1067 cm^{-1}; ^1H- and ^{13}C-NMR: see Tables S2 and S5; HREIMS *m/z* 582.4539, $[M + H]^+$ (calcd for $C_{37}H_{60}NO_4$, 582.4517).

Table 6
The IC_{50} values of the most active antimigratory tocotrienol analogs against the highly metastatic human breast cancer cell line MDA-MB-231 in wound-healing assay.[a]

Compound	IC_{50} (μM)
1	>40.0
2	>40.0
10	1.3
12	8.1
13	6.0
26	4.5
27	2.4
35	10.7
36	2.2
38	1.5
39	4.7
40	4.9
42	7.2

[a] The IC_{50} values are calculated by non-linear regression fitting using GraphPad Prism 5.04. The experiment was conducted in triplicate.

Table 7
Antiproliferative activity (IC_{50}, μM) of selected active tocotrienol analogs against the normal human non-tumorigenic MCF10A mammary epithelial cell line.[a]

Compound	MCF10A	Selectivity index[b]
1	4.4	1.10
13	6.5	3.61
17	8.9	5.24
18	4.6	6.57
23	0.7	0.39
26	8.5	5.67
27	1.9	2.09
36	4.2	2.34
38	2.5	1.92
39	2.0	1.43
40	1.7	2.15

[a] The IC_{50} values are calculated by non-linear regression fitting using GraphPad Prism 5.04.

[b] Values are calculated by dividing the IC_{50} value of each compound against MCF10A normal cells over its IC_{50} value against +SA tumor cells.

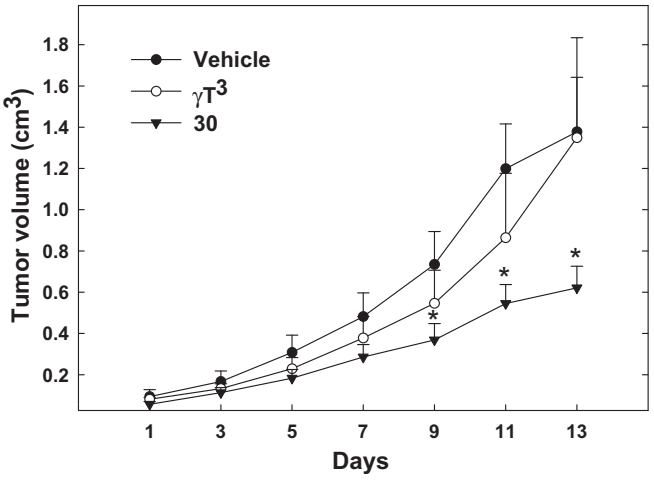

Fig. 6. Effect of daily iv treatment of 0.5 mg of **1** (γT^3) and **30** on +SA mammary tumor growth in intact female syngeneic BALB/c mice throughout a 14-day experimental period. Treatments were initiated around 40 days after 1×10^6 +SA mammary tumor cells were injected into the #4 mammary gland fat pad, when tumors became palpable at approximately 3–5 mm in diameter, and continued for the next 14 days. Data points indicate the average tumor volume (cm^3 ± SEM) for 14–15 mice/treatment group. $^*P < 0.05$, as compared with the vehicle-treated control group.

*4.2.15. (R)-2-(3,3-diethoxypropyl)-6,8-dimethyl-8-((3E,7E)-4,8,12-trimethyltrideca-3,7,11-trienyl)-1,2,3,8,9,10-hexahydrochromeno [5,6-e] [1,3]oxazine (**15**)*

Yellow viscous oil, $[\alpha]_D^{25}$+67.3 (*c* 0.0012, CH_2Cl_2); IR (CH_2Cl_2)ν_{max} 3599, 2922, 2854, 1606, 1374, 1055 cm^{-1}; ^{1}H- and ^{13}C-NMR: see Tables S2 and S5; HREIMS *m/z* 568.4353, $[M + H]^+$ (calcd for $C_{36}H_{58}NO_4$, 568.4360).

*4.2.16. (R)-5,6,8-trimethyl-2-(piperidin-4-ylmethyl)-8-((3E,7E)-4,8,12-trimethyltrideca-3,7,11-trienyl)-1,2,3,8,9,10-hexahydrochromeno[5,6-e] [1,3]oxazine (**16**)*

Yellow viscous oil, $[\alpha]_D^{25}$+0.6 (*c* 0.02, CH_2Cl_2); IR (CH_2Cl_2)ν_{max} 3666, 2922, 2854, 1606, 1521 cm^{-1}; ^{1}H- and ^{13}C-NMR: see Tables S2 and S6; HREIMS *m/z* 549.4392, $[M + H]^+$ (calcd for $C_{36}H_{57}N_2O_2$, 549.4420).

*4.2.17. 5-((R)-5,6,8-trimethyl-8-((3E,7E)-4,8,12-trimethyltrideca-3,7,11-trienyl)-9,10-dihydrochromeno[5,6-e] [1,3]oxazin-2(1H,3H,8H)-yl)pentan-1-ol (**17**)*

Yellow viscous oil, $[\alpha]_D^{25}$+18.4 (*c* 0.0012, CH_2Cl_2); IR (CH_2Cl_2)ν_{max} 3682, 3600, 2929, 2855, 1606, 1378, 1236, 1096 cm^{-1}; ^{1}H- and ^{13}C-NMR: see Tables S2 and S6; HREIMS *m/z* 538.4253, $[M + H]^+$ (calcd for $C_{35}H_{56}NO_3$, 538.4255).

*4.2.18. 5-((R)-6,8-dimethyl-8-((3E,7E)-4,8,12-trimethyltrideca-3,7,11-trienyl)-9,10-dihydrochromeno[5,6-e] [1,3]oxazin-2(1H,3H,8H)-yl)pentan-1-ol (**18**)*

Yellow viscous oil, $[\alpha]_D^{25}$+0.2 (*c* 0.046, CH_2Cl_2); IR (CH_2Cl_2)ν_{max} 3679, 3600, 2929, 2855, 1606, 1473 cm^{-1}; ^{1}H- and ^{13}C-NMR: see Tables S2 and S6; HREIMS *m/z* 524.4109, $[M + H]^+$ (calcd for $C_{34}H_{54}NO_3$, 524.4098).

*4.2.19. 5-((R)-5,6,8-trimethyl-8-((3E,7E)-4,8,12-trimethyltrideca-3,7,11-trienyl)-9,10-dihydrochromeno[5,6-e] [1,3]oxazin-2(1H,3H,8H)-yl)pentanoic acid (**19**)*

Yellow viscous oil, $[\alpha]_D^{25}$+0.2 (*c* 0.04, CH_2Cl_2); IR (CH_2Cl_2)ν_{max} 3683, 3601, 2927, 2854, 1750, 1606, 1465 cm^{-1}; ^{1}H- and ^{13}C-NMR: see Tables S2 and S6; HREIMS *m/z* 552.4033, $[M + H]^+$ (calcd for $C_{35}H_{54}NO_4$, 552.4047).

*4.2.20. 5-((R)-6,8-dimethyl-8-((3E,7E)-4,8,12-trimethyltrideca-3,7,11-trienyl)-9,10-dihydrochromeno[5,6-e] [1,3]oxazin-2(1H,3H,8H)-yl)pentanoic acid (**20**)*

Yellow viscous oil, $[\alpha]_D^{25}$+0.2 (*c* 0.05, CH_2Cl_2); IR (CH_2Cl_2)ν_{max} 3676, 3599, 2927, 2855, 1748, 1606, 1473 cm^{-1}; ^{1}H- and ^{13}C-NMR: see Tables S2 and S6; HREIMS *m/z* 538.3873, $[M + H]^+$ (calcd for $C_{34}H_{52}NO_4$, 538.3891).

*4.2.21. 6-((R)-5,6,8-trimethyl-8-((3E,7E)-4,8,12-trimethyltrideca-3,7,11-trienyl)-9,10-dihydrochromeno[5,6-e] [1,3]oxazin-2(1H,3H,8H)-yl)hexanoic acid (**21**)*

Yellow viscous oil, $[\alpha]_D^{25}$+0.5 (*c* 0.063, CH_2Cl_2); IR (CH_2Cl_2)ν_{max} 3684, 3600, 2930, 2856, 1748, 1606, 1458, 1093 cm^{-1}; ^{1}H- and ^{13}C-NMR: see Tables S2 and S6; HREIMS *m/z* 566.4198, $[M + H]^+$ (calcd for $C_{36}H_{56}NO_4$, 566.4204).

*4.2.22. 6-((R)-6,8-dimethyl-8-((3E,7E)-4,8,12-trimethyltrideca-3,7,11-trienyl)-9,10-dihydrochromeno[5,6-e] [1,3]oxazin-2(1H,3H,8H)-yl)hexanoic acid (**22**)*

Yellow viscous oil, $[\alpha]_D^{25}$+0.2 (*c* 0.05, CH_2Cl_2); IR (CH_2Cl_2)ν_{max} 3676, 3598, 2922, 2855, 1748, 1606, 1473, 1096 cm^{-1}; ^{1}H- and ^{13}C-NMR: see Tables S3 and S6; HREIMS *m/z* 552.4043, $[M + H]^+$ (calcd for $C_{35}H_{54}NO_4$, 552.4047).

*4.2.23. (R)-2-(3,4-dimethoxyphenethyl)-5,6,8-trimethyl-8-((3E,7E)-4,8,12-trimethyltrideca-3,7,11-trienyl)-1,2,3,8,9,10-hexahydrochromeno[5,6-e] [1,3]oxazine (**23**)*

Yellow viscous oil, $[\alpha]_D^{25}$+0.1 (*c* 0.036, CH_2Cl_2); IR (CH_2Cl_2)ν_{max} 3683, 3600, 2921, 2855, 1606, 1516, 1085 cm^{-1}; ^{1}H- and ^{13}C-NMR: see Tables 1 and 3; HREIMS *m/z* 616.4366, $[M + H]^+$ (calcd for $C_{40}H_{58}NO_4$, 616.4360).

*4.2.24. (R)-2-(3,4-dimethoxyphenethyl)-6,8-dimethyl-8-((3E,7E)-4,8,12-trimethyltrideca-3,7,11-trienyl)-1,2,3,8,9,10-hexahydrochromeno[5,6-e] [1,3]oxazine (**24**)*

Yellow viscous oil, $[\alpha]_D^{25}$+0.3 (*c* 0.083, CH_2Cl_2); IR (CH_2Cl_2)ν_{max} 3682, 3600, 2917, 2854, 1606, 1516, 1029 cm^{-1}; ^{1}H- and ^{13}C-NMR: see Tables S3 and S6; HREIMS *m/z* 602.4192, $[M + H]^+$ (calcd for $C_{39}H_{56}NO_4$, 602.4204).

*4.2.25. (R)-3-(3,4-dimethoxyphenethyl)-5,7-dimethyl-7-((3E,7E)-4,8,12-trimethyltrideca-3,7,11-trienyl)-2,3,4,7,8,9-hexahydrochromeno[7,6-e] [1,3]oxazine (**25**)*

Yellow viscous oil, $[\alpha]_D^{25}$+0.3 (*c* 0.013, CH_2Cl_2); IR (CH_2Cl_2)ν_{max} 3676, 2922, 2854, 1606, 1521, 1068, 953 cm^{-1}; ^{1}H- and ^{13}C-NMR: see Tables S3 and S6; HREIMS *m/z* 602.4204, $[M + H]^+$ (calcd for $C_{39}H_{56}NO_4$, 602.4204).

*4.2.26. 4-(2-((R)-5,6,8-trimethyl-8-((3E,7E)-4,8,12-trimethyltrideca-3,7,11-trienyl)-9,10-dihydrochromeno[5,6-e] [1,3] oxazin-2(1H,3H,8H)-yl)ethyl)phenol (**26**)*

Yellow viscous oil, $[\alpha]_D^{25}$+0.6 (*c* 0.026, CH_2Cl_2); IR (CH_2Cl_2)ν_{max} 3676, 3656, 2922, 2855, 1606, 1516, 1083 cm^{-1}; ^{1}H- and ^{13}C-NMR: see Tables 1 and 3; HREIMS *m/z* 572.4090, $[M + H]^+$ (calcd for $C_{38}H_{54}NO_3$, 572.4098).

*4.2.27. 4-(2-((R)-6,8-dimethyl-8-((3E,7E)-4,8,12-trimethyltrideca-3,7,11-trienyl)-9,10-dihydrochromeno[5,6-e] [1,3]oxazin-2(1H,3H,8H)-yl)ethyl)phenol (**27**)*

Yellow viscous oil, $[\alpha]_D^{25}$+2.0 (*c* 0.033, CH_2Cl_2); IR (CH_2Cl_2)ν_{max} 3688, 3599, 2932, 2850, 1606, 1516, 1172 cm^{-1}; ^{1}H- and ^{13}C-NMR: see Tables S3 and S7; HREIMS *m/z* 558.3925, $[M + H]^+$ (calcd for $C_{37}H_{52}NO_3$, 558.3942).

*4.2.28. (R)-5,6,8-trimethyl-2-(3-nitrobenzyl)-8-((3E,7E)-4,8,12-trimethyltrideca-3,7,11-trienyl)-1,2,3,8,9,10-hexahydrochromeno [5,6-e] [1,3]oxazine (**28**)*

Yellow viscous oil, $[\alpha]_D^{25}$ +22.5 (*c* 0.00067, CH_2Cl_2); IR (CH_2Cl_2) ν_{max} 3656, 2922, 2854, 1606, 1531, 1083 cm^{-1}; ^{1}H- and ^{13}C-NMR: see Tables S3 and S7; HREIMS *m/z* 587.3826, $[M + H]^+$ (calcd for $C_{37}H_{51}N_2O_4$, 587.3843).

*4.2.29. (R)-6,8-dimethyl-2-(3-nitrobenzyl)-8-((3E,7E)-4,8,12-trimethyltrideca-3,7,11-trienyl)-1,2,3,8,9,10-hexahydrochromeno [5,6-e] [1,3]oxazine (**29**)*

Yellow viscous oil, $[\alpha]_D^{25}$ +2.8 (*c* 0.013, CH_2Cl_2); IR (CH_2Cl_2)ν_{max} 3676, 3599, 2922, 2854, 1606, 1540, 1374, 1084 cm^{-1}; ^{1}H- and ^{13}C-NMR: see Tables S3 and S7; HREIMS *m/z* 573.3669, $[M + H]^+$ (calcd for $C_{36}H_{49}N_2O_4$, 573.3687).

*4.2.30. 4-((R)-5,6,8-trimethyl-8-((3E,7E)-4,8,12-trimethyltrideca-3,7,11-trienyl)-9,10-dihydrochromeno[5,6-e] [1,3]oxazin-2(1H,3H,8H)-yl)butan-1-ol (**35**)*

Yellow viscous oil, $[\alpha]_D^{25}$ + 8.4 (*c* 0.00166, CH_2Cl_2); IR (CH_2Cl_2)ν_{max} 3434, 2926, 1641, 1464, 1377, 1094, 954 cm^{-1}; ^{1}H- and ^{13}C-NMR: see Tables S3 and S7; HREIMS *m/z* 524.4095, $[M + H]^+$ (calcd for $C_{34}H_{54}NO_3$, 524.4098).

*4.2.31. 4-((R)-6,8-dimethyl-8-((3E,7E)-4,8,12-trimethyltrideca-3,7,11-trienyl)-9,10-dihydrochromeno[5,6-e] [1,3]oxazin-2(1H,3H,8H)-yl)butan-1-ol (**36**)*

Yellow viscous oil, $[\alpha]_D^{25}$ + 10.6 (*c* 0.01133, CH_2Cl_2); IR (CH_2Cl_2) ν_{max} 3210, 2923, 1473, 1379, 1058, 859 cm^{-1}; ^{1}H- and ^{13}C-NMR: see Tables S3 and S7; HREIMS *m/z* 510.3936, $[M + H]^+$ (calcd for $C_{33}H_{52}NO_3$, 510.3941).

*4.2.32. 6-((R)-5,6,8-trimethyl-8-((3E,7E)-4,8,12-trimethyltrideca-3,7,11-trienyl)-9,10-dihydrochromeno[5,6-e] [1,3]oxazin-2(1H,3H,8H)-yl)hexan-1-ol (**37**)*

Yellow viscous oil, $[\alpha]_D^{25}$+8.0 (*c* 0.0114, CH_2Cl_2); IR (CH_2Cl_2)ν_{max} 3617, 2924, 1465, 1378, 1095, 950 cm^{-1}; ^{1}H- and ^{13}C-NMR: see Tables S4 and S7; HREIMS *m/z* 552.4410, $[M + H]^+$ (calcd for $C_{36}H_{58}NO_3$, 552.4411).

*4.2.33. 6-((R)-6,8-dimethyl-8-((3E,7E)-4,8,12-trimethyltrideca-3,7,11-trienyl)-9,10-dihydrochromeno[5,6-e] [1,3]oxazin-2(1H,3H,8H)-yl)hexan-1-ol (**38**)*

Yellow viscous oil, $[\alpha]_D^{25}$+12.6 (*c* 0.019, CH_2Cl_2); IR (CH_2Cl_2)ν_{max} 3616, 2916, 1473, 1379, 1070, 1046, 939, 859 cm^{-1}; ^{1}H- and ^{13}C-NMR: see Tables S4 and S8; HREIMS *m/z* 538.4252, $[M + H]^+$ (calcd for $C_{35}H_{56}NO_3$, 538.4254).

*4.2.34. 8-((R)-5,6,8-trimethyl-8-((3E,7E)-4,8,12-trimethyltrideca-3,7,11-trienyl)-9,10-dihydrochromeno[5,6-e] [1,3]oxazin-2(1H,3H,8H)-yl)octan-1-ol (**39**)*

Yellow viscous oil, $[\alpha]_D^{25}$+7.5 (*c* 0.013, CH_2Cl_2); IR (CH_2Cl_2)ν_{max} 3617, 2922, 1465, 1378, 1096, 950, 845 cm^{-1}; ^{1}H- and ^{13}C-NMR: see Tables S4 and S8; HREIMS *m/z* 580.4718, $[M + H]^+$ (calcd for $C_{38}H_{62}NO_3$, 580.4724).

*4.2.35. 8-((R)-6,8-dimethyl-8-((3E,7E)-4,8,12-trimethyltrideca-3,7,11-trienyl)-9,10-dihydrochromeno[5,6-e] [1,3]oxazin-2(1H,3H,8H)-yl)octan-1-ol (**40**)*

Yellow viscous oil, $[\alpha]_D^{25}$+7.7 (*c* 0.03223, CH_2Cl_2); IR (CH_2Cl_2)ν_{max} 3616, 2909, 1473, 1379, 1073, 1043, 940, 859 cm^{-1}; ^{1}H- and ^{13}C-NMR: see Tables S4 and S8; HREIMS *m/z* 566.4561, $[M + H]^+$ (calcd for $C_{37}H_{60}NO_3$, 566.4567).

*4.2.36. 10-((R)-5,6,8-trimethyl-8-((3E,7E)-4,8,12-trimethyltrideca-3,7,11-trienyl)-9,10-dihydrochromeno[5,6-e] [1,3]oxazin-2(1H,3H,8H)-yl)decan-1-ol (**41**)*

Yellow viscous oil, $[\alpha]_D^{25}$+10.0 (*c* 0.0008, CH_2Cl_2); IR (CH_2Cl_2)ν_{max} 3615, 2928, 1463, 1378, 1098, 950, 846 cm^{-1}; ^{1}H- and ^{13}C-NMR: see Tables S4 and S8; HREIMS *m/z* 608.5064, $[M + H]^+$ (calcd for $C_{40}H_{66}NO_3$, 608.5037).

*4.2.37. 10-((R)-6,8-dimethyl-8-((3E,7E)-4,8,12-trimethyltrideca-3,7,11-trienyl)-9,10-dihydrochromeno[5,6-e] [1,3]oxazin-2(1H,3H,8H)-yl)decan-1-ol (**42**)*

Yellow viscous oil, $[\alpha]_D^{25}$+7.7 (*c* 0.0056, CH_2Cl_2); IR (CH_2Cl_2)ν_{max} 3613, 2927, 1683, 1472, 1378, 1046, 860 cm^{-1}; ^{1}H- and ^{13}C-NMR: see Tables S4 and S8; HREIMS *m/z* 594.4893, $[M + H]^+$ (calcd for $C_{39}H_{64}NO_3$, 594.4881).

*4.2.38. 12-((R)-5,6,8-trimethyl-8-((3E,7E)-4,8,12-trimethyltrideca-3,7,11-trienyl)-9,10-dihydrochromeno[5,6-e] [1,3]oxazin-2(1H,3H,8H)-yl)dodecan-1-ol (**43**)*

Yellow viscous oil, $[\alpha]_D^{25}$+0.5 (*c* 0.00213, CH_2Cl_2); IR (CH_2Cl_2)ν_{max} 3614, 3427, 2928, 1463, 1379, 1098, 950, cm^{-1}; ^{1}H- and ^{13}C-NMR: see Tables S4 and S8; HREIMS *m/z* 636.5361, $[M + H]^+$ (calcd for $C_{42}H_{70}NO_3$, 636.5350).

*4.2.39. 12-((R)-6,8-dimethyl-8-((3E,7E)-4,8,12-trimethyltrideca-3,7,11-trienyl)-9,10-dihydrochromeno[5,6-e] [1,3]oxazin-2(1H,3H,8H)-yl)dodecan-1-ol (**44**)*

Yellow viscous oil, $[\alpha]_D^{25}$+7.7 (*c* 0.00246, CH_2Cl_2); IR (CH_2Cl_2)ν_{max} 3616, 2909, 1473, 1379, 1073, 1043, 940, 859 cm^{-1}; ^{1}H- and ^{13}C-NMR: see Tables S4 and S8; HREIMS *m/z* 622.5181, $[M + H]^+$ (calcd for $C_{41}H_{68}NO_3$, 622.5194).

*4.3. General procedure for the preparation of the Mannich bases (**30** and **31**)*

Each of compounds **23** and **26** was individually dissolved in 75% aqueous methanol and left for 48 h at room temperature with shaking (125 rpm). The solution was concentrated in vacuum and then extracted with dichloromethane (3 × 100 mL). The organic solvent was then evaporated under vacuum and the residue purified using column chromatography. The yield of hydrolysis was 15 and 20%, respectively (Scheme 1c).

*4.3.1. (R)-5-((3,4-dimethoxyphenethylamino)methyl)-2,7,8-trimethyl-2-((3E,7E)-4,8,12-trimethyltrideca-3,7,11-trienyl) chroman-6-ol (**30**)*

Yellow viscous oil, $[\alpha]_D^{25}$+6.0 (*c* 0.0013, CH_2Cl_2); IR (CH_2Cl_2)ν_{max} 3623, 3158, 2923, 1591, 1514, 1381, 1094, 855 cm^{-1}; ^{1}H- and ^{13}C-NMR: see Tables 2 and 3; HREIMS *m/z* 604.4371, $[M + H]^+$ (calcd for $C_{39}H_{58}N\ O_4$, 604.4360).

*4.3.2. (R)-5-((4-hydroxyphenethylamino)methyl)-2,7,8-trimethyl-2-((3E,7E)-4,8,12-trimethyltrideca-3,7,11-trienyl)chroman-6-ol (**31**)*

Yellow viscous oil, $[\alpha]_D^{25}$ +6.7 (*c* 0.0127, CH_2Cl_2); IR (CH_2Cl_2)ν_{max} 3582, 3322, 2917, 1612, 1513, 1379, 1173, 1095, 913 cm^{-1}; ^{1}H- and ^{13}C-NMR: see Tables 2 and 3; HREIMS *m/z* 560.4108, $[M + H]^+$ (calcd for $C_{37}H_{54}NO_3$, 560.4098).

*4.4. General procedure for the preparation of **32**–**34***

To a toluene solution [27] of each of tocotrienols **1** and **2** (25 mmol, 5 mL), acetic acid (0.5 mL), boric acid (40 mmol), and paraformaldehyde (2.4 g) were added. The mixture was refluxed overnight at rt. The reaction was stopped by cooling and washing with cold water, followed by vigorous shaking with a Na_2CO_3

aqueous solution (5% W/V) for 0.5 h, to decompose boric acid complex. Finally, the mixture was washed with water, dried over anhydrous Na_2SO_4, and concentrated under vacuum. The residue was subjected to column chromatography using normal phase Si gel 60 as a stationary phase using gradient *n*-hexane/ethyl acetate system as a mobile phase (Scheme 1d).

*4.4.1. (R)-5-(hydroxymethyl)-2,7,8-trimethyl-2-((3E,7E)-4,8,12-trimethyltrideca-3,7,11-trienyl)chroman-6-ol (**32**)*

Yellow viscous oil, $[\alpha]_D^{25}$+3.0 (*c* 0.05, CH_2Cl_2); IR (CH_2Cl_2)ν_{max} 3590, 3385, 2927, 1620, 1470, 890 cm^{-1}; ^{1}H- and ^{13}C-NMR: see Tables 2 and 3; EIMS *m*/*z* = 423.1.

*4.4.2. (R)-5-(hydroxymethyl)-2,8-dimethyl-2-((3E,7E)-4,8,12-trimethyltrideca-3,7,11-trienyl)chroman-6-ol (**33**)*

Yellow viscous oil, $[\alpha]_D^{25}$+2.6 (*c* 0.048, CH_2Cl_2); IR (CH_2Cl_2)ν_{max} 3595, 3393, 2922, 1607, 1469, 1378, 860 cm^{-1}; ^{1}H- and ^{13}C-NMR: see Tables 2 and 3; HREIMS *m*/*z* 425.3055, [M − H]+ (calcd for $C_{28}H_{41}O_3$, 425.3061).

*4.4.3. (R)-7-(hydroxymethyl)-2,8-dimethyl-2-((3E,7E)-4,8,12-trimethyltrideca-3,7,11-trienyl)chroman-6-ol (**34**)*

Yellow viscous oil, $[\alpha]_D^{25}$+0.9 (*c* 0.0066, CH_2Cl_2); IR (CH_2Cl_2)ν_{max} 3588, 3393, 2924, 1467, 1100, 985 cm^{-1}; ^{1}H- and ^{13}C-NMR: see Tables 2 and 3; HREIMS *m*/*z* 425.3074, [M − H]+ (calcd for $C_{28}H_{41}O_3$, 425.3061).

4.5. Biological assays

4.5.1. In vivo activities

4.5.1.1. +SA cell line. All materials were purchased from Sigma Chemical Company (St. Louis, MO) unless otherwise stated. The highly malignant +SA mouse mammary epithelial cell lines were serially passaged at subconfluent cell density. The +SA mammary tumor cell line was derived from an adenocarcinoma that developed spontaneously in a BALB/c female mouse [33]. Cell culture conditions have been previously described in detail [34]. Briefly, +SA cells were maintained in serum-free defined medium consisting of Dulbecco's modified Eagle's medium (DMEM)/F12 containing 5 mg/mL bovine serum albumin (BSA), 10 mg/mL transferrin, 100 U/mL soybean trypsin inhibitor, 100 U/mL penicillin G, 0.1 mg/mL streptomycin, 10 mg/mL insulin, and 10 ng/mL epidermal growth factor. For subculturing, cells were rinsed twice with sterile Ca^{2+} and Mg^{2+}-free phosphate buffered saline (PBS) and incubated in 0.05% trypsin containing 0.025% EDTA in PBS for 5 min at 37 °C. The released cells were centrifuged, resuspended in fresh media and counted using hemocytometer. A stock solution of the compounds was prepared in DMSO. Once dissolved, this solution was added to a small volume of sterile 10% BSA in water and incubated overnight at 37 °C. This solution conjugated to BSA was used to prepare various concentrations (0–40 μM) of tocotrienol analogs. DMSO was added to all treatment media such that the final DMSO concentration was the same in all treatment groups within a given experiment and was always less than 0.1%.

+SA mammary epithelial cell viable number was determined by the 3-(4,5-dimethylthiazol-2yl)-2,5-diphenyl tetrazolium bromide (MTT) colorimetric assay as described previously [34,35]. Briefly, on the assay day, treatment medium was replaced with fresh control medium containing 0.42 mg/mL MTT, and the cells in 24-well plates were incubated at 37 °C for 4 h. The medium was removed, and the MTT crystals were dissolved in isopropyl alcohol (1 mL/well). The optical density of each sample was read at 570 nm on a microplate reader (SpectraCount, Packard BioScience Company), against a blank prepared from cell-free cultures. The number of cells/well was calculated against a standard curve prepared by plating various concentrations of cells, as determined by hemocytometer, at the start of each experiment [35]. Non-linear regression analysis of treatment effects on viable cell number was used to determine the 50% growth inhibition concentration (IC_{50}) for individual treatments using GraphPad Prism 5.04.

4.5.1.2. MDA-MB-231 and MCF7 human breast cancer cell lines. The antiproliferative effects of tocotrienol analogs on the highly metastatic MDA-MB-231 and MCF7 human cancer cell lines are evaluated as previously described with some modifications [9]. MDA-MB-231 and MCF7 cells were plated at a density of 8×10^3 cells/well and 10^4 cell/well in 96-well culture plates, respectively. The compounds were fed in serum-free media containing 5% and 1% fetal bovine serum for MDA-MB-231 and MCF7 cells, respectively.

4.5.1.3. MCF10A normal human non-tumorigenic mammary epithelial cells. MCF10A (ATCC cat # CRL-10317) cells were maintained in serum-free defined medium consisting of Dulbecco's modified Eagle's medium (DMEM)/F12 containing 5% horse serum, 1% penicillin/streptomycin, 0.5 μg/mL hydrocortisone, 100 ng/mL cholera toxin, 10 μg/mL insulin, and 20 ng/mL epidermal growth factor (rhEGF). For subculturing, cells were rinsed twice with sterile Ca^{2+}- and Mg^{2+}-free phosphate buffered saline (PBS) and incubated in 0.25% trypsin containing 0.025% EDTA in PBS for 5 min at 37 °C. The released cells were centrifuged, resuspended in fresh media and counted using hemocytometer. For testing, MCF10A cells were plated at a density of 10×10^4 cells/well. A stock solution of the compounds was prepared in DMSO. DMSO was added to all treatment media such that the final DMSO concentration was the same in all treatment groups within a given experiment and was always less than 0.1%. The compounds were fed in serum-free media. MCF10A mammary epithelial cell's viable number was determined by MTT colorimetric assay as previously described [9,34,35].

4.5.1.4. NCI-60 human tumor cell line panel. The human tumor cell lines [36–38] of the cancer screening panel are grown in RPMI 1640 medium containing 5% fetal bovine serum and 2 mM L-glutamine. For a typical screening experiment, cells are inoculated into 96-well microtiter plates in 100 μL at plating densities ranging from 5000 to 40,000 cells/well depending on the doubling time of individual cell lines. After cell inoculation, the microtiter plates are incubated at 37 °C, 5% CO_2, 95% air and 100% relative humidity for 24 h prior to addition of experimental drugs. After 24 h, two plates of each cell line are fixed *in situ* with TCA, to represent a measurement of the cell population for each cell line at the time of the addition of the drug (T0). Experimental drugs are solubilized in dimethyl sulfoxide at 400-fold the desired final maximum test concentration and stored frozen prior to use. At the time of drug addition, an aliquot of frozen concentrate is thawed and diluted to twice the desired final maximum test concentration with complete medium containing 50 μg/mL gentamicin. Additional four, 10-fold serial dilutions are made to provide a total of five concentrations plus control. Aliquot of 100 μL of this drug dilution is added to the appropriate microtiter wells already containing 100 μL of medium, resulting in the required final drug concentrations. Following drug addition, the plates are incubated for an additional 48 h at 37 °C, 5% CO_2, 95% air, and 100% relative humidity. For adherent cells, the assay is terminated by the addition of cold TCA. Cells are fixed *in situ* by the gentle addition of 50 μL of cold 50% (w/v) TCA (final concentration, 10% TCA) and incubated for 60 min at 4 °C. The supernatant is discarded, and the plates are washed five times with tap water and air dried. Sulforhodamine B (SRB) solution (100 μL) at 0.4% (w/v) in 1% acetic acid is added to each well, and plates are incubated for 10 min at room temperature. After staining, unbound dye is removed by washing five times with 1% acetic acid and the plates

are air dried. Bound stain is subsequently solubilized with 10 mM trizma base, and the absorbance is read on an automated plate reader at a wavelength of 515 nm. For suspension cells, the methodology is the same except that the assay is terminated by fixing settled cells at the bottom of the wells by gently adding 50 μL of 80% TCA (final concentration, 16% TCA). GI_{50} is the concentration of test drug where $100 \times (T - T0)/(C - T0) = 50$. Where T is the optical density of the test well after a 48-h period of exposure to test drug, $T0$ is the optical density at time zero, and C is the control optical density. The GI_{50} is a measure of the growth inhibitory power of the test agent.

4.5.1.5. Wound-healing assay. The highly metastatic human [7] MDA-MB-231 breast cancer cells were cultured in RPMI 1640 medium containing 10 mM HEPES, 4 mM L-glutamine, 10% fetal bovine serum, penicillin (100 IU/mL), and streptomycin (50 μg/mL), and grown in a 5% CO_2 atmosphere at 37 °C. Cells were plated onto sterile 24-well and allowed to recover for a confluent cell monolayer formed in each well (>95% confluence). Wounds were then inflicted to each cell monolayer using a sterile 200 μL pipette tip. Media were removed, cells were washed twice with PBS, and then fresh media containing test compounds were added to each well. Test compounds were prepared in DMSO at five non-toxic concentrations, each in triplicate using DMSO as negative control. The incubation was carried out for 24 h under low serum-content conditions (0.5%), after which media was removed and cells were fixed and stained using Diff Quick staining (Dade Behring Diagnostics, Aguada, Puerto Rico). The number of cells migrated on the scratched wound were counted under the microscope in three or more randomly selected fields (magnification: 40×). Final results are expressed as mean ± SEM per 40× field.

4.5.2. In vitro activity

4.5.2.1. Tumor implantation into mammary fat pads of syngeneic BALB/c mice. The malignant +SA mammary epithelial cell line was derived from an adenocarcinoma that developed spontaneously in a female BALB/c mouse [33,39]. These cells can be grown on plastic in culture and display the ability to grow in soft agarose [33,39]. Re-implantation of +SA mammary tumor cells back into the mammary fat pad of syngeneic mice results in the rapid develop and growth of metastatic tumors [33,39]. Prior to experimentation, +SA cells were serially passaged at subconfluent cell density. For subculturing, cells are rinsed with calcium/magnesium-free phosphate buffered saline (PBS) and incubated in 0.05% trypsin containing 0.025% EDTA in PBS for 5 min at 37°. The released cells are then diluted in DMEM/F12 media and pelleted by centrifugation. Cell pellets are then resuspended in control culture media, counted by hemocytometer, and then plated at the desired density in culture plates. Cells were then fed fresh media every other day. On the day of tumor implantation, +SA cells grown in culture are isolated with trypsin, washed, counted and diluted to the desired concentration in fresh culture medium. Female BALB/c mice, 3–4 months old were purchased from Harlan Sprague–Dawley (Indianapolis, IN) and housed in plastic cages in a temperature-regulated (24 ± 0.5°) and light-controlled (14 h light/10 h dark) room and allowed standard laboratory mouse chow and water *ad libitum*. At the time of experimentation, animals were anesthetized with an *ip* injection of ketamine/xylazine (10 mg ketamine: 1 mg xylazine/mL saline, Henry Schein, Inc, Melville, NY) at a dose of 0.1 mL/10 g *bw*. A small incision was then made in the skin along the midline of the abdomen, and 1×10^6 cells/0.1 mL culture medium was injected into the #4 mammary gland fat pad (1 tumor/mouse). The incision was then closed, animals allowed to recover, and then returned to their treatment group cages. Approximately 40 days after transplantation, tumors became palpable at an average size of approximately 0.5 mm in diameter. Tumor bearing mice were then divided into the following treatment groups: (1) vehicle-treated controls; (2) 0.5 mg of compound **1** in 0.1 mL of propylene glycol/DMSO (1:1) vehicle; and (3) 0.5 mg of compound **30** in 0.1 mL of propylene glycol/DMSO (1:1) vehicle. Treatments were administered daily by tail vein injection throughout the entire 14 day experimental period. Tumor size and body weighs were recorded every other day. Average tumor diameter for each palpable tumor was determined using the mean of the two largest perpendicular diameters as measured with vernier calipers as previously described [33,39–41]. Tumor volume was determined using the equation:

$$\text{Volume} = \text{Length (cm)} \times \text{Width}^2 \text{ (cm)}/2 \text{ or } V = L \times W^2/2$$

Statistical differences between treatment groups were determined using analysis of variance, followed by Duncan's multiple range test. A difference of $p < 0.05$ was considered to be significant, as compared to the vehicle-treated control group.

Acknowledgments

This publication was supported in part by First Tech International Ltd. (Hong Kong). The Developmental Therapeutics Program – National Cancer Institute (NCI), Bethesda Maryland, is acknowledged for the growth inhibitory screening assays of some compounds.

Appendix A. Supplementary data

Supplementary data related to this article can be found at http://dx.doi.org/10.1016/j.ejmech.2012.11.012.

References

[1] W.G. Burton, Proc. Nutr. Soc. 53 (1994) 251–262.
[2] R. Eitenmiller, J. Lee, Vitamin E: Food Chemistry, Composition, and Analysis, Marcel Dekker Inc., New York, Basil, 2004.
[3] A. Kamal-Eldin, L. Appelqvist, Lipids 31 (1996) 671–701.
[4] L. Packer, S.U. Weber, G. Rimbach, J. Nutr. 131 (2001) 369S–373S.
[5] C.K. Sen, S. Khanna, S. Roy, Life Sci. 78 (2006) 2088–2098.
[6] J.P. Kamat, T.P.A. Devasagayam, Neurosci. Lett. 195 (1995) 179–182.
[7] F.A. Behery, A.Y. Elnagar, M.R. Akl, V.B. Wali, B. Abuasal, A. Kaddoumi, P.W. Sylvester, K.A. El Sayed, Bioorg. Med. Chem. 18 (2010) 8066–8075.
[8] J. Neuzil, K. Kågedal, L. Andera, C. Weber, U.T. Brunk, Apoptosis 7 (2002) 177–185.
[9] A.Y. Elnagar, V.B. Wali, P.W. Sylvester, K.A. El Sayed, Bioorg. Med. Chem. 18 (2010) 755–768.
[10] J. Neuzil, M. Tomasetti, Y. Zhao, L.F. Dong, M. Birringer, X.F. Wang, P. Low, K. Wu, B.A. Salvatore, S. Ralph, J. Mol. Pharmacol. 71 (2007) 1185–1199.
[11] Y. Yano, H. Satoh, K. Fukumoto, I. Kumadaki, T. Ichikawa, K. Yamada, K. Hagiwara, T. Yano, Int. J. Cancer 115 (2005) 839–846.
[12] N. Akaho, J. Takata, T. Fukushima, K. Matsunaga, A. Hattori, R. Hidaka, K. Fukui, M. Yoshida, T. Fujioka, Y. Karube, K. Imai, Drug Metab. Dispos. 35 (2007) 1502–1510.
[13] M. Birringer, J.H. EyTina, B.A. Salvatore, J. Neuzil, Br. J. Cancer 88 (2003) 1948–1955.
[14] F.F. Blicke, Organic Reactions, John Wiley and Sons, Inc., New York, 1942.
[15] T. Nakamura, S. Kijima, Chem. Pharm. Bull. 19 (1971) 2318–2324.
[16] W.J. Burke, J. Am. Chem. Soc. 71 (1949) 609–612.
[17] W.J. Burke, R.P. Smith, C. Weatherbee, J. Am. Chem. Soc. 74 (1952) 602–605.
[18] M. Tramontini, Synthesis 12 (1973) 703–775.
[19] M. Tramontini, L. Angiolini, Tetrahedron 46 (1990) 1791–1837.
[20] D. Shi, S. Rong, G. Dou, M. Wang, J. Comb. Chem. 12 (2010) 25–30.
[21] J.B. Chylinska, T. Urbanski, M. Mordarski, J. Med. Chem. 6 (1963) 484–487.
[22] L. Benameur, Z. Bouaziz, P. Nebois, M. Bartoli, M. Boitard, H. Fillion, Chem. Pharm. Bull. 44 (1996) 605–608.
[23] S. Wang, Y. Li, Y. Liu, A. Lu, Q. You, Bioorg. Med. Chem. Lett. 18 (2008) 4095–4097.
[24] B.P. Mathew, A. Kumar, S. Sharma, P.K. Shukla, M. Nath, Eur. J. Med. Chem. 45 (2010) 1502–1507.
[25] L. Cappannini, C. Cimarelli, S. Giuli, G. Palmieri, M. Petrini, Tetrahedron Asymm. 18 (2007) 1022–1029.
[26] W.J. Burke, C.W. Stephens, J. Am. Chem. Soc. 74 (1952) 1518–1520.
[27] T. Nakamura, S. Kijima, Chem. Pharm. Bull. 20 (1972) 1681–1686.
[28] S. Ohnmacht, R. West, R. Simionescu, J. Atkinson, Magn. Reson. Chem. 46 (2008) 287–294.
[29] B.S. McIntyre, K.P. Briski, A. Gabor, P.W. Sylvester, Proc. Soc. Exp. Biol. Med. 224 (2000) 292–301.

[30] H.K. Liu, Q. Wang, Y. Li, W.G. Sun, J.R. Liu, Y.M. Yang, W.L. Xu, X.R. Sun, B.Q. Chen, J. Nutr. Biochem. 21 (2010) 206–213.
[31] P.N. Chang, W.N. Yap, D.T. Lee, M.T. Ling, Y.C. Wong, Y.L. Yap, Nutr. Cancer 61 (2009) 357–366.
[32] W.N. Yap, P.N. Chang, H.Y. Han, D.T.W. Lee, M.T. Ling, Y.C. Wong, Y.L. Yap, Br. J. Cancer 99 (2008) 1832–1841.
[33] L.W. Anderson, K.G. Danielson, H.L. Hosick, In Vitro 15 (1979) 841–843.
[34] V.B. Wali, P.W. Sylvester, Lipids 42 (2007) 1113–1123.
[35] P.W. Sylvester, H.P. Birkenfeld, H.L. Hosick, K.P. Briski, Exp. Cell. Res. 214 (1994) 145–153.
[36] M.R. Boyd, K.D. Paull, L.R. Rubinstein, in: F.A. Vleriote, T.H. Corbett, L.H. Baker (Eds.), Cytotoxic Anticancer Drugs: Models and Concepts for Drug Discovery and Development, Kluwer Academic, Hingham, MA, 1992, pp. 11–34.
[37] M.R. Grever, S.A. Sehepartz, B.A. Chabners, Semin. Oncol. 19 (1992) 622–638.
[38] A. Monks, D. Schudiero, P. Skehan, R. Shoemaker, K. Paull, D. Vistica, C. Hose, J. Langley, P. Cronise, A. Vaigro-Wolff, M. Gray-Goodrich, H. Campbell, J. Mayo, M. Boyd, J. Natl. Cancer Inst. 83 (1991) 757–766.
[39] K.G. Danielson, L.W. Anderson, H.L. Hosick, Cancer Res. 40 (1980) 1812–1819.
[40] P.W. Sylvester, M. Russell, M.M. Ip, C. Ip, Cancer Res. 46 (1986) 757–762.
[41] P.W. Sylvester, C. Ip, M.M. Ip, Cancer Res. 46 (1986) 763–769.